tvst

https://doi.org/10.1167/tvst.7.6.12

Article

Effects of Age, Race, and Ethnicity on the Optic Nerve and Peripapillary Region Using Spectral-Domain OCT 3D Volume Scans

Linda Yi-Chieh Poon[1,2], Hussein Antar[1,3], Edem Tsikata[1], Rong Guo[1,4], Georgia Papadogeorgou[5,6], Madeline Freeman[1,7], Ziad Khoueir[1,8], Ramon Lee[1,9], Eric Shieh[1,10], Huseyin Simavli[1,11], Christian John Que[1,12], Johannes F. de Boer[13,14], and Teresa C. Chen[1]

[1] Department of Ophthalmology, Glaucoma Service, Massachusetts Eye and Ear Infirmary, Harvard Medical School, Boston, MA, USA
[2] Department of Ophthalmology, Kaohsiung Chang Gung Memorial Hospital, Chang Gung University College of Medicine, Kaohsiung, Taiwan
[3] University of Massachusetts Medical School, Worcester, MA, USA
[4] Department of Medicine, University of California, Los Angeles, CA, USA
[5] Department of Biostatistics, Harvard T.H. Chan School of Public Health, Boston, MA, USA
[6] Department of Statistical Science, Duke University, Durham, NC, USA
[7] Smith College School for Social Work, Northampton, MA, USA
[8] Beirut Eye and ENT Specialist Hospital, Université Saint-Joseph Medical School, Beirut, Lebanon
[9] University of Southern California Roski Eye Institute, Department of Ophthalmology, Keck School of Medicine, University of Southern California, Los Angeles, CA, USA
[10] Jules Stein Eye Institute, David Geffen School of Medicine, University of California, Los Angeles, CA, USA
[11] Department of Ophthalmology, Pamukkale University, School of Medicine, Denizli, Turkey
[12] University of the East Ramon Magsaysay Memorial Medical Center, Quezon City, Philippines
[13] LaserLaB, Department of Physics and Astronomy, Vrije Universiteit, Amsterdam, The Netherlands
[14] Department of Ophthalmology, Vrije Universiteit Medical Center, Amsterdam, The Netherlands

Correspondence: Teresa C. Chen, Harvard Medical School, Department of Ophthalmology, Massachusetts Eye and Ear Infirmary, Glaucoma Service, 243 Charles Street, Boston, MA 02114, USA. e-mail: teresa_chen@meei.harvard.edu

Received: 31 May 2018
Accepted: 20 September 2018
Published: 27 November 2018

Keywords: age; aging; optic nerve; peripapillary retina; race; three-dimensional OCT; spectral-domain OCT

Citation: Poon LY-C, Antar H, Tsikata E, Guo R, Papadogeorgou G, Freeman M, Khoueir Z, Lee R, Shieh E, Simavli H, Que CJ, de Boer JF, Chen TC. Effects of age, race, and ethnicity on the optic nerve and peripapillary region using spectral-domain OCT 3D volume scans. Trans Vis Sci Tech. 2018;7(6):12, https://doi.org/10.1167/tvst.7.6.12

Purpose: To evaluate the effects of age, race, and ethnicity on the optic nerve and peripapillary retina using spectral-domain optical coherence tomography (SD-OCT) three-dimensional (3D) volume scans in normal subjects.

Methods: This is a cross-sectional study performed at a single institution in Boston. All patients received retinal nerve fiber layer (RNFL) scans and an optic nerve 3D volume scan. The SD-OCT software calculated peripapillary RNFL thickness, retinal thickness (RT), and retinal volume (RV). Custom-designed software calculated neuroretinal rim minimum distance band (MDB) thickness and area.

Results: There were 272 normal subjects, including 175 whites, 40 blacks, 40 Asians, and 17 Hispanics. Rates of age-related decline were 2.3%, 2.0%, 1.7%, 3.3%, and 4.3% per decade for RNFL, RT, RV, MDB neuroretinal rim thickness, and MDB area, respectively. The RNFL was most affected by racial and ethnic variations, with Asians having thicker global, superior, and inferior RNFL, Hispanics having thicker inferior RNFL, and blacks having thinner temporal RNFL, compared to whites. For MDB thickness and area, Asians had smaller nasal values and blacks had smaller temporal values. Peripapillary RT and RV parameters were not influenced by race and ethnicity.

Conclusions: All of the parameters exhibited age-related declines. RNFL, MDB thickness, and MDB area demonstrated racial and ethnic variations, while peripapillary RT and RV did not.

Translational Relevance: This study demonstrates that both normal aging and ethnicity affect several novel 3D OCT parameters used to diagnose and monitor glaucoma (i.e., RT, RV, and MDB), and this should be factored in when making clinical decisions based on these parameters.

Introduction

Advances in spectral-domain optical coherence tomography (SD-OCT)[1–3] have established optical coherence tomography (OCT) as an integral part of clinical care in glaucoma today.[4–6] This SD-OCT technology not only allows for detailed visualization of the optic nerve and peripapillary retina but also allows for quantifiable and reproducible measurements of these structures.[1,7–10]

The most common OCT parameter used for evaluating glaucomatous structural change is peripapillary two-dimensional (2D) retinal nerve fiber layer (RNFL) thickness,[11–13] which is typically obtained along a 3.45 to 3.46 mm diameter circle centered on the disc. However, as glaucoma progresses, the RNFL reflectivity decreases,[14] causing the border between the RNFL and ganglion cell layer to become less distinct, leading to segmentation errors of the RNFL border. As a result, the artifact rate for peripapillary RNFL scans has been reported to be as high as 19.9%[15] to 46.3%.[16] Therefore, there is a need for other parameters that can be reliably identified while also yielding high diagnostic performance. Several newer parameters of the macula and optic nerve head have been investigated and include macular retinal thickness (RT),[17] macular inner RT,[18] and the neuroretinal rim parameter Bruch's membrane opening-minimum rim width (BMO-MRW).[19] This paper, however, focuses on other, newer parameters, which can be generated from a three-dimensional (3D) volume scan of the optic nerve and its peripapillary region. These 3D optic nerve volume scan parameters include the following: peripapillary RT within an annular region,[20] peripapillary retinal volume (RV) within an annular region,[21] neuroretinal rim minimum distance band (MDB) thickness,[1,22,23] and neuroretinal rim MDB area.[23]

For glaucoma diagnosis, OCT parameters that can be derived from a 3D optic nerve volume scan have been shown to have similar or better diagnostic capability compared to RNFL thickness measurements while sometimes having fewer artifacts.[20–23] For example, peripapillary RT and RV have diagnostic performance that is comparable to or better than RNFL thickness.[20,21] Furthermore, peripapillary RT and RV may have an advantage over RNFL thickness because retinal measurements may have fewer segmentation difficulties, as can be seen with glaucomatous RNFL reflectivity loss and peripapillary atrophy (PPA).[20,21] Similar to the BMO-MRW, the MDB is a 3D neuroretinal rim parameter that quantifies the amount of tissue in the neuroretinal rim band, which is delimited internally by the retinal surface and externally by the OCT-derived disc border, based on the termination of the retinal pigment epithelium/Bruch's membrane (RPE/BM) complex.[1,22,23] The MDB thickness has similar or better diagnostic capability compared to RNFL thickness for glaucoma and performs significantly better in the nasal region,[22,23] which is a region where the RNFL parameter typically yields poorer diagnostic performance.[11,13]

Because new glaucoma OCT parameters derived from 3D volume scans may have the same or better diagnostic capability compared to the traditional 2D RNFL thickness parameter, it is important to know the normal variations of these new 3D volume scan–derived parameters. The primary hypothesis of this study is that age, race, and ethnicity can affect the following OCT parameters in a normal population: RNFL thickness, neuroretinal rim parameters (i.e., MDB thickness and area), and peripapillary retinal parameters (i.e., RT and RV).

Methods

Subjects

Study subjects were prospectively recruited between 2009 and 2015 from the Glaucoma Service of the Massachusetts Eye and Ear Infirmary (MEEI) as a part of the prospective Spectral Domain Optical Coherence Tomography in Glaucoma (SIG) study.[7,11,16,20–23] Informed consents were obtained from all study patients. The study methods were approved by the MEEI Institutional Review Board, adhered to the tenets of the Declaration of Helsinki, and was compliant with the Health Insurance Portability and Accountability Act.

All subjects had a comprehensive eye examination, which included history, visual acuity (VA), refraction, intraocular pressure (IOP), slit lamp biomicroscopy, dilated fundus exam, visual field (VF) testing (Swedish Interactive Threshold Algorithm 24-2 test, Humphrey VF Analyzer; Carl Zeiss Meditec Inc., Dublin, CA), color disc photography (Visucam Pro NM; Carl Zeiss Meditec Inc.), and SD-OCT imaging (Spectralis HRA-OCT; Heidelberg Engineering, Heidelberg, Germany).

Subjects were included in the study if they satisfied all of the following inclusion criteria: (1) age >18 years; (2) clinically normal eye exam except for mild cataracts; (3) IOP of ≤ 21 mm Hg; (4) best-corrected VA of $\geq 20/40$; (5) normal VF results defined by a Glaucoma Hemifield Test that is within normal limits and without a pattern standard deviation that has a probability of

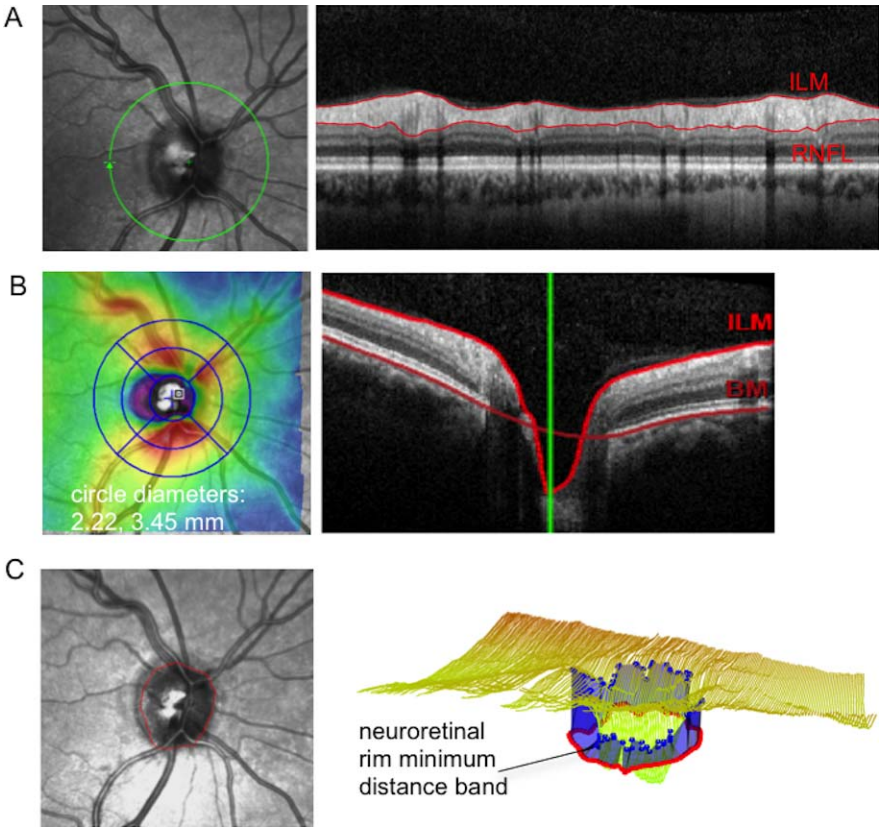

Figure 1. Peripapillary and neuroretinal parameters investigated in this study. (A) Sample of RNFL scan centered on the optic nerve, from which RNFL thickness is obtained for analysis. (B) Illustration of how peripapillary RT and RV were obtained from volume scans of the optic nerve and a RT color map superimposed on the infrared reflectance (IR) image of the peripapillary region, with a circular grid with circle diameters of 1, 2.22, and 3.45 mm manually centered on the optic nerve. The RT and RV values within the outer annulus (2.22–3.45 mm) were analyzed. (C) The OCT-based disc border (*red dots*) superimposed on the IR image of the peripapillary region and a 3D image of the neuroretinal rim MDB generated by our customized software. On the 3D image, *yellow lines* are the segmented internal limiting membrane layer. The *red dots* represent the OCT-based disc border, which correlates with the termination of the RPE/BM complex. The *blue dots* represent the cup surface points closest to the corresponding OCT-based disc border, between which forms the MDB (*blue band*).

occurring in <5% of the normal population; and (6) spherical equivalent between −5 and +5 diopters.

Subjects were excluded from the study if they had (1) unreliable VF test results with >33% fixation loss, >20% false-negative results, or >20% false-positive results; (2) any neurologic disease or use of systemic medication that could produce VF defects; (3) OCT image quality score (Q) of <15 on the RNFL circle scan printout.

Subjects were categorized into the following racial and ethnic categories: white, black, Asian, and Hispanic. The category "black" includes Hispanic blacks, while Hispanic refers only to Hispanic whites. In all cases, racial and ethnic classification are based on self-identification.

Spectralis OCT Scanning

After pupillary dilation, each subject underwent OCT imaging and received two scans centered on the optic nerve: (1) a standard 12° circular scan, which equates to a retinal diameter of approximately 3.46 mm in an eye with typical corneal curvature and axial length, and (2) a 20° × 20° volume scan consisting of 193 equidistant horizontal frames with the automatic real time set to 3.

Analysis of Peripapillary RNFL Thickness and Peripapillary Annulus Parameters

Peripapillary RFNL thickness was determined by the instrument's built-in software, which automatically segments the internal limiting membrane (ILM) and the posterior RNFL border and then determines thickness values as the distance between these two layers (Fig. 1A). The global and four-quadrant RNFL thickness values were used for analysis.

Peripapillary RT and RV values were obtained from 3D volume scans of the optic nerve. To calculate

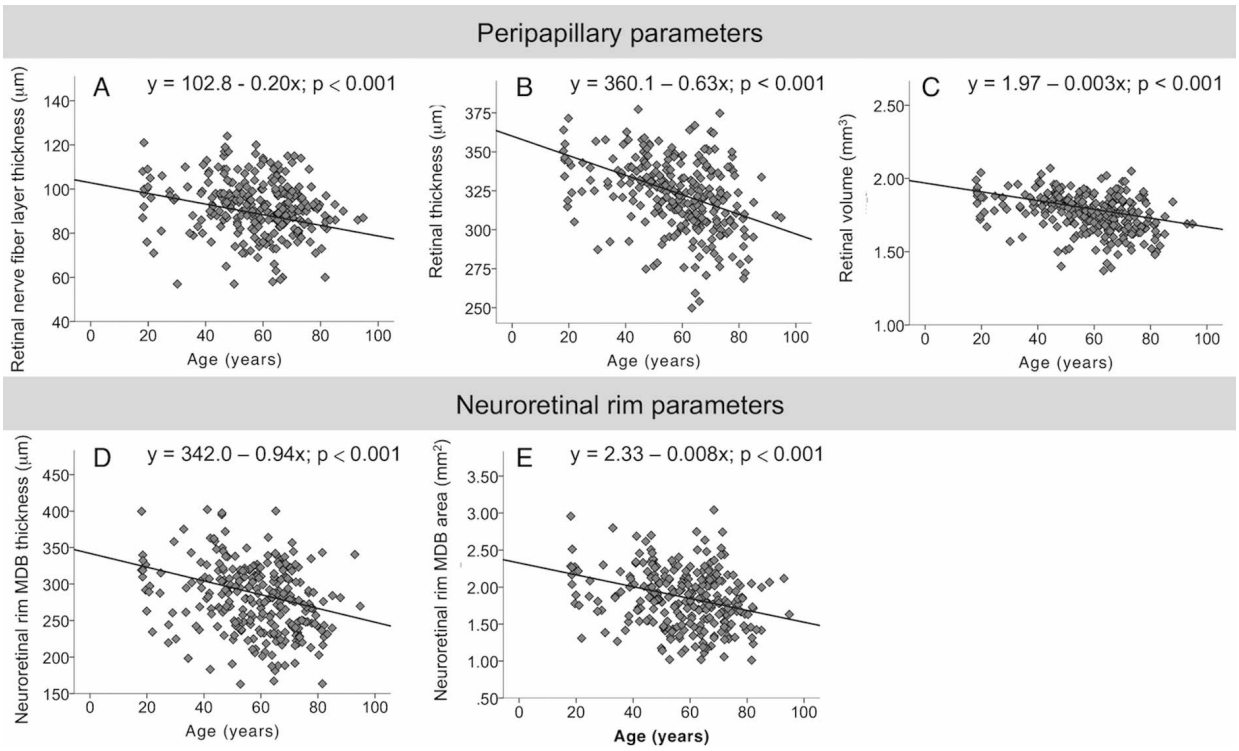

Figure 2. Scatter plots of age versus the global values of three peripapillary parameters and two neuroretinal rim parameters. The three peripapillary parameters are (A) RNFL thickness, (B) RT, and (C) RV. The two neuroretinal rim parameters are (D) MDB thickness and (E) MDB area.

RT and RV within an annular region, Figure 1B shows how the Early Treatment Diabetic Retinopathy Study (ETDRS) circular grid was manually centered over the optic nerve using the machine's built-in software (Heidelberg Eye Explorer, version 1.9.10.0; Heidelberg Engineering). In the example shown (Fig. 2A), the retinal borders were segmented in red, with the anterior retinal border being the ILM and the posterior retinal border being Bruch's membrane.[24] Using the ETDRS circular grid with diameters of 1, 2.22, and 3.45 mm, peripapillary RT and RV values within the outer annulus of this ETDRS circle grid (i.e., inner circle diameter 2.22 mm and outer circle diameter 3.45 mm; Fig. 1B) were obtained for analysis. This annulus diameter was chosen based on our previous work,[20,21] since it yielded higher diagnostic capability for glaucoma compared to a larger annulus of 3 to 6 mm and was less affected by the presence of PPA, compared to a smaller annulus of 2 to 3 mm. The global and four-quadrant values were used for analysis. Global RT values were determined by averaging RT for the four quadrants, and global RV values were generated by the OCT's built-in software.

Analysis of Neuroretinal Rim MDB Parameters

The methods and custom-designed software used to determine MDB thickness and area from 3D optic nerve volume scans were described in prior studies.[22,23] In brief, the custom-designed software was developed at MEEI and used Open Source Computer Vision (version 2.4.3; OpenCV, Willow Garage, Menlo Park, CA) and the Insight Segmentation and Registration Toolkit (ITK, version 4.3; Insight Software Consortium, Kitware Inc., Clifton Park, NY) libraries. This software automatically segments the ILM and the RPE/BM complex, and the segmented images were manually reviewed and corrected for errors. The software then determines the OCT-derived disc margin (i.e., termination of RPE/BM), which is represented by 100 points that are 3.6° apart. The program identifies the 100 closest corresponding points on the ILM, creating a 3D ribbon that is defined as the MDB (Fig. 1C). MDB thickness was calculated as the average of the shortest distance between corresponding points on the ILM and RPE/BM termination. MDB area takes into account the multidirectionality assumed by the 3D

MDB ribbon, and the MDB area is calculated from the summation of the areas of triangles formed by two adjacent points on the ILM or RPE/BM termination and their corresponding shortest point on the ILM or RPE/BM.[23] Global and quadrant MDB neuroretinal rim thickness and area values were obtained for analysis.

Statistical Analysis

One eye from each subject was chosen randomly to be included in the analysis. Statistical analyses were performed using statistical software (SAS 9.4; SAS Institute Inc., Cary, NC, and R 3.2.3). Descriptive statistics were used to report continuous variables as mean ± the standard deviation. Categorical variables were reported as percentages. ANOVA was used for comparison of the mean values between different ethnic groups. The effects of age, race, and ethnicity on each of the parameters were analyzed using multivariate analysis that adjusted for gender and refraction. $P < 0.05$ was considered statistically significant.

Results

OCT images from 272 eyes of 272 subjects were analyzed (Table 1). The average age of subjects was 57.8 ± 15.7 years with a range of 18 to 94 years. All subjects were healthy as defined by the inclusion criteria. The majority of subjects were white (64.3%). The Asian population ($n = 40$) comprised 15 Chinese, 3 Korean, 3 Japanese, 9 Indian, 5 Vietnamese, and 5 unclassified Asian subjects.

Table 2 summarizes the global and quadrant mean values for peripapillary RNFL thickness, peripapillary RT, peripapillary RV, neuroretinal MDB thickness, and neuroretinal rim MDB area. The mean RNFL thickness and neuroretinal rim parameters in general followed the ISNT rule and were thickest in the inferior quadrant, followed by the superior, nasal, and temporal quadrants. Peripapillary RT and RV showed similar trends of having thicker values in the vertical quadrants and thinner values in the horizontal quadrants.

Table 2 also shows the absolute slope for changes with age after adjusting for race and refraction, for all of the parameters. Regionally, RNFL thickness had the highest rate of age-related change in the superior quadrant (–0.35 μm per year, $P < 0.001$). For RT, age-related change was greatest in the inferior quadrant (–0.79 μm per year, $P < 0.001$). Peripapillary RV showed similar rates of decline in most of the quadrants (–0.001 mm^3 per year, $P < 0.001$) but decreased at a slower rate in the temporal quadrant (–0.0003 mm^3 per year, $P = 0.004$). For the neuroretinal rim, MDB thickness demonstrated the highest rate of age-related change in the inferior quadrant (–1.27 μm per year, $P < 0.001$), while for MDB area, similar rates of decline were found in the superior, inferior, and nasal quadrants (–0.002 μm per year for all three quadrants; all $P < 0.05$). Temporal quadrant changed the least with age in all of the parameters and in general demonstrated no statistically significant relationship with age.

Figure 2 shows that the global values for peripapillary RNFL thickness, peripapillary RT, peripapillary RV, neuroretinal rim MDB thickness, and neuroretinal rim MDB area all decreased significantly with age. With respect to the population mean, the rates of age-related change correspond to a decline of 2.3% per decade for RNFL thickness, a 2.0% decline per decade for peripapillary RT, and a 1.7% decline per decade for peripapillary RV (Table 2). While at the neuroretinal rim, MDB thickness exhibits a 3.3% decrease per decade, and the MDB area demonstrates a 4.3% decrease per decade (Table 2).

Figure 3 shows the mean values of peripapillary RNFL thickness, peripapillary RT and RV, and

Table 1. Summary of Patient Demographics

Patient Characteristics	$n = 272$
Age, y, mean ± SD	57.8 ± 15.7
<30 y, *n* (%)	19 (7.0)
30–39 y, *n* (%)	13 (4.8)
40–49 y, *n* (%)	46 (16.9)
50–59 y, *n* (%)	61 (22.4)
60–69 y, *n* (%)	68 (25.0)
70–79 y, *n* (%)	51 (18.8)
>80 y, *n* (%)	14 (5.1)
Female, *n* (%)	158 (58.1)
Right eye, *n* (%)	152 (55.9)
Race and ethnicity, *n* (%)	
White	175 (64.3)
Black	40 (14.7)
Asian	40 (14.7)
Hispanic	17 (6.3)
Spherical equivalent, D, mean ± SD	−0.37 ± 1.79
Mean deviation on HVF, dB, mean ± SD	−1.70 ± 2.08

D, diopters; HVF, Humphrey VF; dB, decibel.

Table 2. Mean Normal Values for OCT Neuroretinal and Peripapillary Parameters: Rates of Age-Related Decline by Absolute Values and by Percentages

OCT Parameters	Mean ± SD	Absolute Slope[a] (95% CI), Unit/Year	*P*	Rate of Decline, %/Decade
Peripapillary parameters				
2D circle scan–RNFL thickness, μm				
Global	91.8 ± 12.4	−0.204 (−0.302 to −0.107)	<0.001	−2.3
Superior	110.3 ± 19.4	−0.354 (−0.505 to −0.202)	<0.001	−3.3
Inferior	118.1 ± 19.3	−0.272 (−0.423 to −0.121)	0.001	−2.8
Nasal	70.7 ± 16.0	−0.195 (−0.323 to −0.067)	0.008	−2.4
Temporal	68.2 ± 13.6	0.005 (−0.106 to 0.116)	0.958	0.1
3D volume scan–RT, μm				
Global	322.4 ± 22.9	−0.628 (−0.806 to −0.451)	<0.001	−2.0
Superior	343.6 ± 28.6	−0.752 (−0.974 to −0.530)	<0.001	−2.2
Inferior	341.8 ± 29.0	−0.793 (−1.016 to −0.569)	<0.001	−2.3
Nasal	303.7 ± 25.6	−0.695 (−0.894 to −0.495)	<0.001	−2.3
Temporal	300.9 ± 28.2	−0.276 (−0.509 to 0.043)	0.046	−0.9
3D volume scan–RV, mm^3				
Global	1.76 ± 0.12	−0.003 (−0.004 to −0.002)	<0.001	−1.7
Superior	0.47 ± 0.04	−0.001 (−0.001 to −0.001)	<0.001	−2.1
Inferior	0.47 ± 0.04	−0.001 (−0.001 to −0.001)	<0.001	−2.2
Nasal	0.42 ± 0.03	−0.001 (−0.001 to −0.001)	<0.001	−2.4
Temporal	0.41 ± 0.03	−0.0003 (−0.001 to −0.0001)	0.004	−0.7
Neuroretinal rim parameters				
3D volume scan–MDB thickness, μm				
Global	279.3 ± 46.6	−0.943 (−1.318 to −0.569)	<0.001	−3.3
Superior	300.4 ± 60.8	−0.975 (−1.480 to −0.469)	0.001	−3.2
Inferior	315.5 ± 61.1	−1.274 (−1.769 to −0.778)	<0.001	−4.0
Nasal	281.3 ± 55.1	−0.945 (−1.387 to −0.503)	<0.001	−3.3
Temporal	221.1 ± 47.9	−0.592 (−0.982 to −0.201)	0.008	−2.6
3D volume scan–MDB area, mm^2				
Global	1.84 ± 0.40	−0.008 (−0.011 to −0.004)	<0.001	−4.3
Superior	0.52 ± 0.15	−0.002 (−0.004 to −0.001)	0.001	−4.0
Inferior	0.54 ± 0.14	−0.002 (−0.004 to −0.001)	<0.001	−3.8
Nasal	0.46 ± 0.13	−0.002 (−0.003 to −0.001)	0.002	−4.2
Temporal	0.33 ± 0.10	−0.001 (−0.002 to 0.0003)	0.059	−2.9

CI, confidence interval.
[a] Adjusted for race and refraction.

MDB neuroretinal rim thickness and area, according to race and ethnicity. Highest variation is present for RNFL thickness values, with the global and most quadrant values showing significant differences between the racial and ethnic groups, while for MDB thickness and area, significant differences between racial and ethnic groups were present for the nasal and temporal quadrant. The least variation is observed for peripapillary RT and RV values, in which no statistical differences were detected for the global and quadrant values for either of these parameters.

Using whites as the reference group, multivariate analysis that adjusted for age and refraction showed that race and ethnicity significantly affected expected normal RNFL thickness values and MDB neuroretinal rim parameters, but not peripapillary retinal parameters (Table 3). RNFL thickness was most affected by race and ethnicity, in which blacks had thinner RNFL thickness values in the temporal

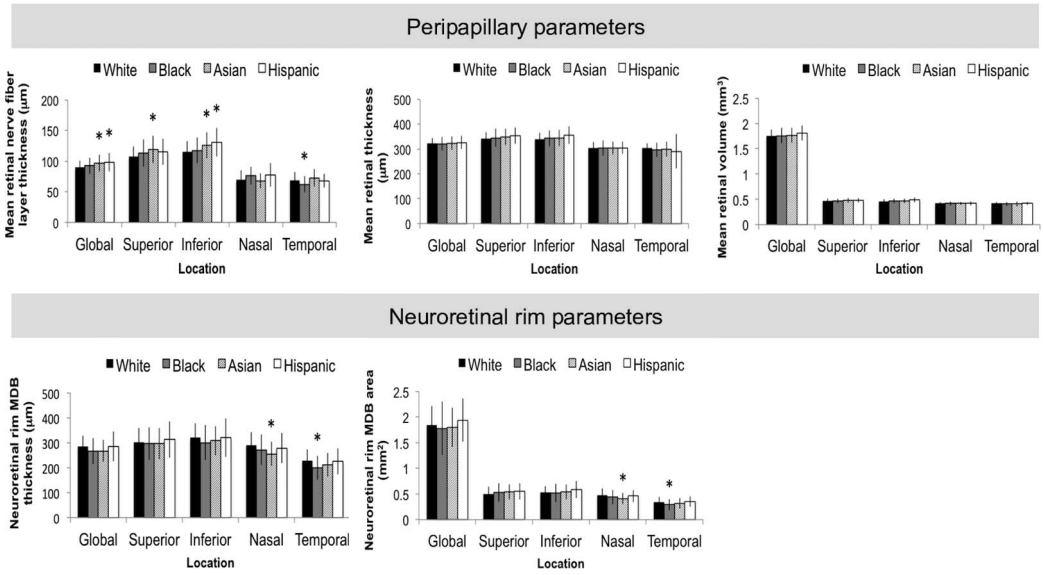

Figure 3. Bar graphs showing the racial and ethnic variations in the mean and standard deviation values of three peripapillary retinal parameters and two neuroretinal rim parameters. *Asterisks* represent significant difference ($P < 0.05$) when compared to white. *Error bars* represent standard deviation.

quadrant; Asians had thicker global, superior, and inferior RNFL thickness values; and Hispanic patients had thicker inferior RNFL thickness values. For the neuroretinal rim parameter, blacks had thinner temporal MDB thickness values and smaller MDB areas, and Asians had smaller MDB thickness and MDB area values in the nasal quadrant. There was no significant racial or ethnic influence on 3D peripapillary retinal parameters.

Discussion

As new parameters from 3D OCT optic nerve volume scans emerge for the diagnosis and long-term monitoring of glaucoma patients, it is important to characterize the effects of aging on these parameters and to understand how these parameters are affected by differing races and ethnicities. Our study is, to our knowledge, the first to comprehensively assess how aging, race, and ethnicity affect not only the traditional 2D RNFL thickness parameter but also the newer 3D OCT volume scan parameters, such as neuroretinal rim MDB thickness, neuroretinal rim MDB area, peripapillary RT, and peripapillary RV, all of which can be derived from a single 3D volume scan of the optic nerve head.

As the most commonly used OCT parameter for the management of glaucoma, the relationship between RNFL thickness and aging in the normal population has been thoroughly investigated in past studies, with decline rates of −1.5 to −3.7 μm per decade being reported.[25–32] In our study, we found a decline rate of −2.0 μm per decade for global RNFL thickness (Table 2), compatible with what was reported in previous studies. With regard to the quadrants, RNFL thickness has been found to be most strongly affected by age in the superior[25,27,29,33] and inferior[26,32] quadrants, similar to the findings in this study, in which highest rates of RNFL age-related change were found in the superior (−3.5 μm per decade, Table 2) and the inferior quadrants (−2.7 μm per decade, Table 2).

To our knowledge, although the age-related changes in the macular retina have been extensively studied in the past,[29,34–40] the effect of aging on the peripapillary retina has not been comprehensively investigated previously. Different from prior studies on global macular retinal thickness, which reported rates of age-related thinning of −1.9 to −4.2 μm per decade,[29,36,38] our study found that global peripapillary RT had age-related decline at a rate of −6.3 μm per decade (Table 2). Although our results are higher than the rates previously reported for the macular retinal thickness, our results are consistent with the fact that a higher proportion of RNFL exists in the peripapillary region, as the RNFL is normally thinner the farther one is from the optic nerve.[31,41] Similar to peripapillary RT, our study also found a higher global peripapillary RV decline of −0.03 mm^3 (−1.7%) per decade (Table 2), compared to other studies of the

Table 3. Linear Regression Analysis Showing the Effects of Race and Ethnicity on the Global and Regional Values of Three Peripapillary Retinal Parameters and Two Neuroretinal Rim Parameters[a,b]

	Black		Asian		Hispanic	
OCT Parameters	β Coefficient	*P*	β Coefficient	*P*	β Coefficient	*P*
Peripapillary parameters						
2D circle scan–RNFL thickness						
Global	1.17	0.684	6.72	0.004*	6.03	0.085
Superior	4.17	0.308	12.14	0.001*	5.44	0.368
Inferior	0.54	0.920	11.21	0.002*	12.76	0.015*
Nasal	5.79	0.067	−1.03	0.820	5.93	0.219
Temporal	−6.11	0.023*	4.06	0.154	−0.04	0.991
3D volume scan–RT						
Global	−4.34	0.381	−1.41	0.820	−0.71	0.934
Superior	−0.77	0.920	3.02	0.643	6.43	0.479
Inferior	−1.30	0.884	0.24	0.979	9.20	0.289
Nasal	−3.43	0.559	−2.97	0.628	−4.01	0.641
Temporal	−7.83	0.191	−5.96	0.354	−14.45	0.085
3D volume scan–RV						
Global	−0.023	0.417	−0.005	0.890	0.024	0.580
Superior	0.000	0.988	0.005	0.546	0.009	0.491
Inferior	−0.001	0.907	0.001	0.931	0.014	0.227
Nasal	−0.004	0.581	−0.002	0.827	−0.004	0.747
Temporal	−0.011	0.098	−0.010	0.154	0.005	0.681
Neuroretinal rim parameters						
3D volume scan–MDB thickness						
Global	−23.17	0.008*	−22.05	0.015*	−7.44	0.641
Superior	−10.28	0.464	−8.02	0.594	3.45	0.900
Inferior	−27.18	0.022*	−17.76	0.159	−9.94	0.641
Nasal	−23.65	0.025*	−40.98	<0.001*	−17.98	0.289
Temporal	−31.57	<0.001*	−20.77	0.029*	−5.72	0.747
3D volume scan–MDB area						
Global	−0.113	0.169	−0.070	0.447	0.021	0.907
Superior	0.008	0.874	0.034	0.313	0.023	0.652
Inferior	−0.027	0.404	−0.002	0.967	0.033	0.491
Nasal	−0.043	0.108	−0.079	0.002*	−0.035	0.417
Temporal	−0.051	0.015*	−0.024	0.320	−0.001	0.988

* *P* values represent statistical significance of $P < 0.05$.
[a] White was used as reference group.
[b] Adjusted for age and refraction.

macular retina that reported global thinning rates corresponding to −0.6%[36] to −0.8%[38] per decade. For quadrants, our study found that the highest age-related change occurred in the superior and inferior quadrants for both peripapillary RT and RV (Table 2). This similar trend was also observed for RNFL thickness in our study, and also in other studies,[25,27,29,33] and shows that the age-related thinning in the peripapillary retina may be associated with the thinning of the RNFL. Therefore, our data not only showed that there are distinct differences between rates of age-related thinning in the peripapillary retina compared to previously reported rates for the macular retina,[29,36–38] it also showed that comprehensive evaluation of age-related changes in both the peripapillary RNFL and the optic nerve fibers requires analyzing the peripapillary retina and not just the macular retina.

Analysis of neuroretinal rim MDB parameters also showed that the neuroretinal rim demonstrates significant changes with age. The neuroretinal rim MDB, as described in our previously published studies,[22,23] is an OCT-derived parameter that represents an encircling band of tissue composed of the retinal nerve fibers as they exit the eye. The neuroretinal rim MDB thickness and area are derived from 3D optic nerve volume scans and provide a surrogate measure of the total amount of nerve tissue in the optic nerve. The MDB determines a neuroretinal rim band and is similar to the BMO-MRW,[19,42] but the MDB differs from the BMO-MRW by defining the OCT-derived disc border as the RPE/BM complex versus just the Bruch's membrane opening.[22,23] Future studies to directly compare the age-related changes of MDB versus BMO-MRW would be interesting. Past histology studies of the optic nerve have demonstrated a loss of 2.9%[43] to 3.7%[44] of axons in the optic nerve per decade, which were comparable to the rates of age-related changes we observed in this study for global MDB thickness at −3.3% per decade, and for global MDB area at −4.3% per decade (Table 2).

Comparison between the global parameters showed that peripapillary parameters (i.e., RNFL thickness at −2.3% per decade; peripapillary RT at −2.0% per decade; peripapillary RV at −1.7% per decade) appeared to proportionally have slower rates of age-related decline than neuroretinal rim parameters (i.e., MDB thickness at −3.3% per decade; MDB area at −4.3% per decade) (Table 2). Similar trends were observed by Chauhan et al.[32] in which a loss of 2.1% per decade was found for RNFL thickness, while BMO-MRW had a loss of 4.0% per decade.[32] The different rates of age-related changes may be explained by the different proportions of retinal ganglion cell (RGC) axons, which exhibit atrophic changes with aging, to supporting glial cells, which have self-renewal properties and remain activated with aging,[45,46] in the peripapillary retina versus the neuroretinal rim. In the neuroretinal rim, which is the region represented by the MDB, about 94% are RGC axons and about 5% are glial contents.[47] In contrast, in the peripapillary retina, the proportion of glial contents in the nerve bundles is about 18% to 35%.[48] Thus, the higher rate of decline observed in the MDB parameters may reflect a higher proportion of RGC axons to glial cells within the neuroretinal rim compared to the peripapillary retina. The clinical relevance of these findings is that through comprehensive 3D analysis of the peripapillary region and the optic nerve, we found that age-related thinning occurs at differing rates depending on the structure being evaluated, and that in normal eyes, the neuroretinal rim demonstrates considerably higher age-related thinning compared to the peripapillary retina and RNFL, which should be regarded as a normal aging process and not mistaken for glaucomatous disease progression.

Our study also found racial and ethnic differences in the OCT parameters that were derived from 3D optic nerve volume scans. For the traditional 2D RNFL thickness parameter (Fig. 3), we found that Hispanics had thicker global and inferior RNFL values compared to whites, which is consistent with the past literature[25,34,49] and may be associated with larger discs in Hispanics compared to whites,[50,51] resulting in thicker RNFL measurements in Hispanics due to the fixed scan circle being closer to the disc border. In our study, we also found that blacks had thinner temporal RNFL thickness (Fig. 3) compared to whites. This is also consistent with what was previously reported in the literature.[34,52] The least racial and ethnic variations were observed for the 3D peripapillary retinal parameters, RT and RV (Fig. 3; Table 3). We suspect that racial and ethnic variations in disc size may have less effect on peripapillary retinal parameters (i.e., RT and RV) compared to the RNFL thickness parameter because any effects of varying disc size may be blunted with peripapillary retinal parameters, which evaluate a wider peripapillary region (i.e., a 2.22 to 3.45 mm annulus) compared to the traditional 2D RNFL thickness parameter. With regard to the neuroretinal rim, we found that, compared to whites, Asians had smaller nasal MDB thickness and area values, while blacks had thinner temporal MDB thickness and area values. This may be due to the relatively larger disc sizes and cupping found in normal Asians and blacks compared to whites.[50,51] Since the MDB measures neuroretinal rim tissue, this parameter may be more greatly affected by racial and ethnic variations in disc morphology. In summary, we found that the RNFL thickness parameter was most affected by racial variations, with blacks having thinner temporal RNFL; Asians having thicker global, superior, and inferior RNFL; and Hispanics having thicker inferior RNFL. For MDB thickness and area, Asians had smaller nasal MDB thickness and area values and blacks had smaller temporal MDB thickness and area values. Peripapillary RT and RV parameters were not affected by race and ethnicity. Thus, our findings suggest that, clinically,

when deciding whether an observed thinning in the RNFL or neuroretinal rim is attributable to glaucoma or not, race and ethnicity should be factored in since artifactual thinning may be attributable to racial and ethnic differences, and this highlights the importance of race- and ethnicity-specific normative databases for these OCT parameters. Peripapillary RT and RV, on the other hand, appears not to be affected by race and ethnicity and thus may be a more useful parameter for monitoring disease progression in a clinical setting where patients of many different races and ethnicities are being examined. BMO-MRW is similar to the MDB OCT parameter and may be useful in a multiracial clinical setting because BMO-MRW was found to have no racial variations in a study comparing subjects of African descent versus European descent.[53]

Our study had a number of limitations. One of the limitations was its cross-sectional study design, where individual variability and sampling bias might have contributed to results that are not necessarily universally generalizable. A second limitation was that there was not an even distribution of races and ethnicities in the study, which included predominantly whites (Table 1). Our study results would therefore need to be interpreted with caution, especially for races and ethnicities with small patient numbers; however, our study findings of racial and ethnic differences in RNFL thickness are consistent with findings in prior studies.[25,34,49,52] Therefore, by extrapolation, this study's findings of the influence of race and ethnicity on certain 3D OCT parameters may still be valid. Another limitation is the categorization of the Asian population in this study, which is comprised of subjects who are Chinese, Korean, Japanese, and Indian. Although often present in the ophthalmic literature, the term "Asian" carries with it an assumption of relative genetic homogeneity, when in fact this may capture a heterogeneous group of people. A better study would have included larger numbers of each Asian subgroup, but the current study of only 40 Asian subjects does not have adequate numbers for subgroup analysis. Additionally, all of the normal subjects in this study were recruited from a university-based glaucoma clinic, and a larger population-based study might have found different results. However, our normal study subjects included a diversity of races and ethnicities similar to the racial composition of the Boston Metropolitan area and had an average cup-to-disc ratio of 0.48, which is not unexpected with a study population with some black and Hispanic subjects, whose cup-to-disc ratios are normally up to 0.6.

In conclusion, this study revealed significant age-related decline in both MDB neuroretinal rim and peripapillary retinal parameters (i.e., RT and RV), with the neuroretinal rim MDB parameters demonstrating the highest rates of age-related decline compared to the other parameters. In terms of normal racial and ethnic variations, RNFL thickness and neuroretinal rim parameters demonstrated the most variation among different races and ethnicities, while the peripapillary RT and RV were not affected by racial and ethnic differences. This study underscores the importance of factoring in age-related changes and ethnic variations when making clinical decisions based on neuroretinal rim and peripapillary retinal OCT parameters in glaucoma management.

Acknowledgments

Supported by American Glaucoma Society Mid-Career Award (TCC), Massachusetts Lions Eye Research Fund (TCC), Fidelity Charitable Fund (TCC), Harvard Catalyst Grant (TCC), National Institutes of Health Grant (TCC; UL RR025758), and Department of Defense Small Business Innovation Research (TCC; DHP15-016).

Disclosure: **L.Y.-C. Poon**, None; **H. Antar**, None; **E. Tsikata**, None; **R. Guo**, None; **G. Papadogeorgou**, None; **M. Freeman**, None; **Z. Khoueir**, None; **R. Lee**, None; **E. Shieh**, None; **H. Simavli**, None; **C.J. Que**, None; **J.F. de Boer**, Center for Biomedical Optical Coherence Tomography Research and Translation Scientific Advisory Board Chair, Harvard Medical School (S), licenses to NIDEK, Inc., Terumo Corporation, Ninepoint Medical, and Heidelberg Engineering (F); **T.C. Chen**, None

References

1. Chen TC. Spectral domain optical coherence tomography in glaucoma: qualitative and quantitative analysis of the optic nerve head and retinal nerve fiber layer (an AOS thesis). *Trans Am Ophthalmol Soc*. 2009;107:254–281.
2. Chen TC, Cense B, Pierce MC, et al. Spectral domain optical coherence tomography: ultra-high

speed, ultra-high resolution ophthalmic imaging. *Arch Ophthalmol*. 2005;123:1715–1720.
3. Folio LS, Wollstein G, Schuman JS. Optical coherence tomography: future trends for imaging in glaucoma. *Optom Vis Sci*. 2012;89:E554–562.
4. Chauhan BC, Burgoyne CF. From clinical examination of the optic disc to clinical assessment of the optic nerve head: a paradigm change. *Am J Ophthalmol*. 2013;156:218–227.
5. Grewal DS, Tanna AP. Diagnosis of glaucoma and detection of glaucoma progression using spectral domain optical coherence tomography. *Curr Opin Ophthalmol*. 2013;24:150–161.
6. Bussel II, Wollstein G, Schuman JS. OCT for glaucoma diagnosis, screening and detection of glaucoma progression. *Br J Ophthalmol*. 2014; 98(suppl 2):ii15–19.
7. Wu H, de Boer JF, Chen TC. Reproducibility of retinal nerve fiber layer thickness measurements using spectral domain optical coherence tomography. *J Glaucoma*. 2011;20:470–476.
8. Matlach J, Wagner M, Malzahn U, Gobel W. Repeatability of peripapillary retinal nerve fiber layer and inner retinal thickness among two spectral domain optical coherence tomography devices. *Invest Ophthalmol Vis Sci*. 2014;55:6536–6546.
9. Menke MN, Dabov S, Knecht P, Sturm V. Reproducibility of retinal thickness measurements in healthy subjects using spectralis optical coherence tomography. *Am J Ophthalmol*. 2009; 147:467–472.
10. Suh MH, Yoo BW, Park KH, Kim H, Kim HC. Reproducibility of spectral-domain optical coherence tomography RNFL map for glaucomatous and fellow normal eyes in unilateral glaucoma. *J Glaucoma*. 2015;24:238–244.
11. Wu H, de Boer JF, Chen TC. Diagnostic capability of spectral-domain optical coherence tomography for glaucoma. *Am J Ophthalmol*. 2012;153:815–826.
12. Leung CK, Cheung CY, Weinreb RN, et al. Retinal nerve fiber layer imaging with spectral-domain optical coherence tomography: a variability and diagnostic performance study. *Ophthalmology*. 2009;116:1257–1263.
13. Leung CK, Lam S, Weinreb RN, et al. Retinal nerve fiber layer imaging with spectral-domain optical coherence tomography: analysis of the retinal nerve fiber layer map for glaucoma detection. *Ophthalmology*. 2010;117:1684–1691.
14. van der Schoot J, Vermeer KA, de Boer JF, Lemij HG. The effect of glaucoma on the optical attenuation coefficient of the retinal nerve fiber layer in spectral domain optical coherence tomography images. *Invest Ophthalmol Vis Sci*. 2012;53:2424–2430.
15. Asrani S, Essaid L, Alder BD, Santiago-Turla C. Artifacts in spectral-domain optical coherence tomography measurements in glaucoma. *JAMA Ophthalmol*. 2014;132:396–402.
16. Liu Y, Simavli H, Que CJ, et al. Patient characteristics associated with artifacts in Spectralis optical coherence tomography imaging of the retinal nerve fiber layer in glaucoma. *Am J Ophthalmol*. 2015;159:565–576.
17. Zeimer R, Asrani S, Zou S, Quigley H, Jampel H. Quantitative detection of glaucomatous damage at the posterior pole by retinal thickness mapping. A pilot study. *Ophthalmology*. 1998;105: 224–231.
18. Mwanza JC, Durbin MK, Budenz DL, et al. Glaucoma diagnostic accuracy of ganglion cell-inner plexiform layer thickness: comparison with nerve fiber layer and optic nerve head. *Ophthalmology*. 2012;119:1151–1158.
19. Chauhan BC, O'Leary N, Almobarak FA, et al. Enhanced detection of open-angle glaucoma with an anatomically accurate optical coherence tomography-derived neuroretinal rim parameter. *Ophthalmology*. 2013;120:535–543.
20. Simavli H, Que CJ, Akduman M, et al. Diagnostic capability of peripapillary retinal thickness in glaucoma using 3D volume scans. *Am J Ophthalmol*. 2015;159:545–556.
21. Simavli H, Poon LY, Que CJ, et al. Diagnostic capability of peripapillary retinal volume measurements in glaucoma. *J Glaucoma*. 2017;26: 592–601.
22. Shieh E, Lee R, Que C, et al. Diagnostic performance of a novel three-dimensional neuroretinal rim parameter for glaucoma using high-density volume scans. *Am J Ophthalmol*. 2016; 169:168–178.
23. Tsikata E, Lee R, Shieh E, et al. Comprehensive three-dimensional analysis of the neuroretinal rim in glaucoma using high-density spectral-domain optical coherence tomography volume scans. *Invest Ophthalmol Vis Sci*. 2016;57:5498–5508.
24. Heidelberg Engineering GmbH. *SPECTRALIS HRA+OCT User Manual, Software Version 6.0*. Heidelberg, Germany: Heidelberg Engineering; 2014.
25. Alasil T, Wang K, Keane PA, et al. Analysis of normal retinal nerve fiber layer thickness by age, sex, and race using spectral domain optical coherence tomography. *J Glaucoma*. 2013;22: 532–541.

26. Celebi AR, Mirza GE. Age-related change in retinal nerve fiber layer thickness measured with spectral domain optical coherence tomography. *Invest Ophthalmol Vis Sci*. 2013;54:8095–8103.
27. Parikh RS, Parikh SR, Sekhar GC, Prabakaran S, Babu JG, Thomas R. Normal age-related decay of retinal nerve fiber layer thickness. *Ophthalmology*. 2007;114:921–926.
28. Harwerth RS, Wheat JL, Rangaswamy NV. Age-related losses of retinal ganglion cells and axons. *Invest Ophthalmol Vis Sci*. 2008;49:4437–4443.
29. Sung KR, Wollstein G, Bilonick RA, et al. Effects of age on optical coherence tomography measurements of healthy retinal nerve fiber layer, macula, and optic nerve head. *Ophthalmology*. 2009;116:1119–1124.
30. Patel NB, Lim M, Gajjar A, Evans KB, Harwerth RS. Age-associated changes in the retinal nerve fiber layer and optic nerve head. *Invest Ophthalmol Vis Sci*. 2014;55:5134–5143.
31. Hirasawa H, Tomidokoro A, Araie M, et al. Peripapillary retinal nerve fiber layer thickness determined by spectral-domain optical coherence tomography in ophthalmologically normal eyes. *Arch Ophthalmol*. 2010;128:1420–1426.
32. Chauhan BC, Danthurebandara VM, Sharpe GP, et al. Bruch's membrane opening minimum rim width and retinal nerve fiber layer thickness in a normal white population: A sulticenter study. *Ophthalmology*. 2015;122:1786–1794.
33. Leung CK, Yu M, Weinreb RN, et al. Retinal nerve fiber layer imaging with spectral-domain optical coherence tomography: a prospective analysis of age-related loss. *Ophthalmology*. 2012;119:731–737.
34. Girkin CA, McGwin G Jr, Sinai MJ, et al. Variation in optic nerve and macular structure with age and race with spectral-domain optical coherence tomography. *Ophthalmology*. 2011; 118:2403–2408.
35. Duan XR, Liang YB, Friedman DS, et al. Normal macular thickness measurements using optical coherence tomography in healthy eyes of adult Chinese persons: the Handan Eye Study. *Ophthalmology*. 2010;117:1585–1594.
36. Patel PJ, Foster PJ, Grossi CM, et al. Spectral-domain optical coherence tomography imaging in 67,321 adults: associations with macular thickness in the UK Biobank Study. *Ophthalmology*. 2016;123:829–840.
37. Song WK, Lee SC, Lee ES, Kim CY, Kim SS. Macular thickness variations with sex, age, and axial length in healthy subjects: a spectral domain-optical coherence tomography study. *Invest Ophthalmol Vis Sci*. 2010;51:3913–3918.
38. Gupta P, Sidhartha E, Tham YC, et al. Determinants of macular thickness using spectral domain optical coherence tomography in healthy eyes: the Singapore Chinese Eye study. *Invest Ophthalmol Vis Sci*. 2013;54:7968–7976.
39. Wang J, Gao X, Huang W, et al. Swept-source optical coherence tomography imaging of macular retinal and choroidal structures in healthy eyes. *BMC Ophthalmol*. 2015;15:122.
40. Adhi M, Aziz S, Muhammad K, Adhi MI. Macular thickness by age and gender in healthy eyes using spectral domain optical coherence tomography. *PLoS One*. 2012;7:e37638.
41. Varma R, Skaf M, Barron E. Retinal nerve fiber layer thickness in normal human eyes. *Ophthalmology*. 1996;103:2114–2119.
42. Reis AS, O'Leary N, Yang H, et al. Influence of clinically invisible, but optical coherence tomography detected, optic disc margin anatomy on neuroretinal rim evaluation. *Invest Ophthalmol Vis Sci*. 2012;53:1852–1860.
43. Jonas JB, Schmidt AM, Muller-Bergh JA, Schlotzer-Schrehardt UM, Naumann GO. Human optic nerve fiber count and optic disc size. *Invest Ophthalmol Vis Sci*. 1992;33:2012–2018.
44. Mikelberg FS, Drance SM, Schulzer M, Yidegiligne HM, Weis MM. The normal human optic nerve. Axon count and axon diameter distribution. *Ophthalmology*. 1989;96:1325–1328.
45. Karlstetter M, Langmann T. Microglia in the aging retina. *Adv Exp Med Biol*. 2014;801:207–212.
46. Johnson EC, Morrison JC. Friend or foe? Resolving the impact of glial responses in glaucoma. *J Glaucoma*. 2009;18:341–353.
47. Minckler DS, McLean IW, Tso MO. Distribution of axonal and glial elements in the rhesus optic nerve head studied by electron microscopy. *Am J Ophthalmol*. 1976;82:179–187.
48. Ogden TE. Nerve fiber layer of the primate retina: thickness and glial content. *Vision Res*. 1983;23:581–587.
49. Knight OJ, Girkin CA, Budenz DL, Durbin MK, Feuer WJ, Cirrus OCTNDSG. Effect of race, age, and axial length on optic nerve head parameters and retinal nerve fiber layer thickness measured by Cirrus HD-OCT. *Arch Ophthalmol*. 2012;130: 312–318.
50. Lee RY, Kao AA, Kasuga T, et al. Ethnic variation in optic disc size by fundus photography. *Curr Eye Res*. 2013;38:1142–1147.

51. Seider MI, Lee RY, Wang D, Pekmezci M, Porco TC, Lin SC. Optic disk size variability between African, Asian, white, Hispanic, and Filipino Americans using Heidelberg retinal tomography. *J Glaucoma*. 2009;18:595–600.
52. Girkin CA, Sample PA, Liebmann JM, et al. African Descent and Glaucoma Evaluation Study (ADAGES): II. Ancestry differences in optic disc, retinal nerve fiber layer, and macular structure in healthy subjects. *Arch Ophthalmol*. 2010;128:541–550.
53. Rhodes LA, Huisingh CE, Quinn AE, et al. Comparison of Bruch's membrane opening minimum rim width among those with normal ocular health by race. *Am J Ophthalmol*. 2017;174:113–118.